INSTITUTE OF PHYSICS PUBLISHING JOURNAL OF PHYSICS B: ATOMIC, MOLECULAR AND OPTICAL PHYSICS

J. Phys. B: At. Mol. Opt. Phys. **37** (2004) 4239–4257 PII: S0953-4075(04)84897-1

High resolution kinetic energy release spectra and angular distributions from double ionization of nitrogen and oxygen by short laser pulses

S Voss, A S Alnaser, X-M Tong, C Maharjan, P Ranitovic, B Ulrich, B Shan, Z Chang, C D Lin and C L Cocke

J R Macdonald Laboratory, Physics Department, Kansas State University, Manhattan, KS 66506, USA

E-mail: cocke@phys.ksu.edu

Received 11 August 2004
Published 26 October 2004
Online at stacks.iop.org/JPhysB/37/4239
doi:10.1088/0953-4075/37/21/002

Abstract

We have used momentum imaging techniques to measure in high resolution the kinetic energy release spectra and angular distributions of coincident O^+ and N^+ ion pairs produced by short laser pulses (8–35 fs) on targets of N_2 and O_2 at peak intensities between 1 and 12 $\times$ 10^{14} W cm^{-2}. We record the full momentum vectors of both members of each pair and achieve a kinetic energy release resolution of less than 0.3 eV. We find that the process proceeds through well-defined electronic states of the excited molecular dications. Using linear and circularly polarized light, we identify two mechanisms for the production of these states, rescattering and sequential ionization. By using 8 fs pulses, we observe that the internuclear distance can be frozen during the pulse. For low intensities and 8 fs pulses, emission from N_2 is strongly directed along the polarization vector, while that for O_2 is not, a result we interpret as being due to the different symmetries of the outer orbitals of these molecules. For high intensities and longer pulses, the distributions increasingly fold towards the polarization vector, ultimately peaking at zero degrees for both molecules. For oxygen, a local peaking for molecules aligned at right angles to the polarization vector is seen. A discussion and interpretation of the results are presented.

(Some figures in this article are in colour only in the electronic version)

Introduction

The production of ions from the interaction of intense laser pulses with neutral molecules has been widely studied over the past decade. It was established early that for laser pulses long enough to allow the fragments to move during the pulse, the kinetic energy release was

much less than would be expected if the fragments simply Coulomb exploded from their initial equilibrium positions [1–14]. This was interpreted in terms of the now well-established (charge resonance) enhanced ionization [15–24] process, whereby the molecule expands until the ionization rate reaches a maximum. This occurs at a distance substantially larger than the equilibrium one, releasing considerably less kinetic energy than a Coulomb explosion from the equilibrium separation would. An alternative explanation for the kinetic energy release (KER) deficit in terms of screening of the Coulomb force during the explosion process by the electron charge has also been proposed [25–27], and no clear resolution of this discussion seems to have appeared in the literature. The full ionization process is in any case complex, requiring a combination of successive ionizations which take place at the same time the molecule is expanding.

In this paper we examine the KER spectra from the diatomic molecules O_2 and N_2, focusing only on the final channel which results in the production of pairs of singly charged ions. These fragments result from the creation of excited doubly charged molecules which are almost certainly the precursors of all higher charged molecules. Thus an understanding of the mechanisms for production of these ion pairs stands the possibility of helping considerably in unravelling the overall process. A major issue which must be addressed immediately is: how does the molecule become electronically excited? Successive ionization through removal of electrons from the outermost orbitals via a tunnelling process will not result in dissociative states of these molecules because of the bonding effects of the many remaining electrons. On the basis of our KER spectra, and their dependence on pulse length, field strength and polarization, we suggest different pathways through which this may occur.

Laser fragmentation of these molecules has been reported by several authors previously for pulses ranging from ps [28, 29] to tens of fs [30–35] and treated theoretically in [36, 37]. The KER spectra have generally been deduced from time-of-flight spectra of fragments measured along the extraction field directions of electrostatic spectrometers. Such an approach gives good KER centroids, but has not given high KER resolution allowing the dissociative states involved to be identified. The most comprehensive attempt to follow the evolution of the N_2 molecule through its several ionization stages was made by Nibarger *et al* [30], who proposed a model for attaining higher charge states, starting with dissociative states of the doubly charged molecule. In this paper we address the question: how does the molecule get into these states in the first place?

This question is also closely related to the question of how the alignment of the molecule with respect to the laser polarization vector affects the ionization rate, which we also investigate in this paper. The first step in the multiple ionization of molecules by short intense laser pulses is the extraction, usually via a tunnelling process, of an electron from the most loosely bound orbital in the molecule. While the extraction of electrons from atomic targets is well described over a large range of laser intensities by ADK tunnelling theory [38] as well as by *ab initio* solutions to Schrödinger's equation, such calculations for molecules are less advanced and more problematic. Recently a simple application of ADK theory to molecules has been proposed by Tong *et al* [39]. They exploit the fact that the asymptotic form of the molecular orbitals resembles atomic states with assignable quantum numbers to apply ADK formulae to molecules. Using this approach, they were able to account for the long-standing puzzle that the single ionization of O_2 is suppressed relative to that of N_2 [40–45]. This formalism has the advantage of simplicity and accessibility. Other explanations have involved interference between outgoing electron wave packets generated from the two centres with a relative phase also associated with the symmetry of the outermost orbitals [46–50]. All these explanations inherently predict that the ionization rate from the neutral molecule should depend strongly

on the symmetry properties of the orbital from which the electron is extracted and thus on the alignment of the molecule with respect to the laser field.

Clean experimental verification of this prediction has been problematic. Whereas many experiments on the angular distributions of dissociation products from molecules exposed to strong laser pulses have been reported (for a review, see [51]), these do not generally show exactly what is needed to test the angular dependence predicted by the molecular ADK or any other model for ionization. The ideal experiment would be to align the neutral molecule by some independent process and then to measure the ionization rate as a function of the angle θ between the molecule and the polarization vector. N_2 and O_2 are particularly interesting molecules with which to explore this question because they have very different outer orbital symmetries and the molecular ADK predicts very different angular dependences of the ionization rate on angle for these molecules. The outermost orbital of N_2 is a $3\sigma_g$, for which the ionization should peak at $\theta = 0$; for O_2, it is a π_g, for which the rate should peak near $\theta = 45^\circ$. Recently Litvinyuk *et al* [52] proposed, and exploited, a novel method of aligning molecules. They used rotational wave packets generated by a short pump pulse to cause the molecule to align at well-determined times after this pulse. They were able to achieve sufficient control over the alignment of N_2 to measure with confidence the ionization rate as a function of θ, and found that this rate peaked strongly near $\theta = 0$, as predicted by the molecular ADK. A similar measurement on O_2 was inconclusive, however. More recently Légaré *et al* [53] have shown harmonic generation from O_2 peaks when the molecule is not along the laser polarization, a result expected from the molecular ADK prediction for O_2.

Here we present measurements of the angular distributions of ion fragments from the double ionization of O_2 and N_2 by short (8–35 fs) pulses. The original idea behind this study was to see if we could see evidence for the different angular patterns predicted by the molecular ADK for these molecules in the theta dependence of the N^+/N^+ or O^+/O^+ pair distributions. Since at least two, maybe more, steps are involved in reaching the observed double ionization channel, and the initial ionization is only the first step, it is not at all clear that such evidence will not be masked by angular dependences of later steps. However, measurements on H_2 [54, 55] showed that, for very low laser intensities, where rescattering ionization/excitation of the intermediate H_2^+ ion was the dominant process, the angular distribution of ion pairs was nearly isotropic. This implied that both the single ionization and the subsequent rescattering ionization/excitation were nearly isotropic, a result in agreement with expectations. For H_2 the initial wavefunction is nearly isotropic asymptotically, and the rescattering process would not *a priori* be expected to be strongly angular dependent. Therefore we thought it is quite possible that, in the low intensity region where rescattering is the dominant mechanism for ion-pair formation, the angular dependence of the initial ionization step might persist in the ion-pair distribution as well. That is, the subsequent steps might have weaker angular dependence. (We note that the Keldysh parameter for single ionization of these molecules passes unity below 10^{14} W cm^{-2}, and thus it is sensible to describe the first electron removal as a tunnelling process). We show in this paper that this expectation is to a considerable extent born out. We also show that the angular distributions change their character completely when one raises the laser power into the sequential ionization regime. A brief account of this aspect has been published in [56]; here we present a more comprehensive discussion.

Experiment

We use coincident momentum imaging techniques, often referred to in the literature as COLTRIMS, to determine the full momentum vectors of both singly charged ions on an event-by-event basis. The technique is described in detail in [57, 58]. A schematic of the

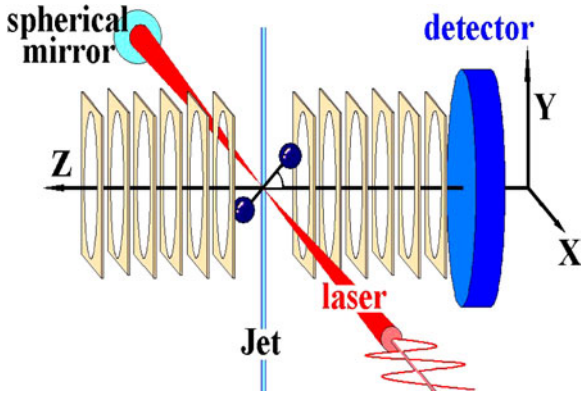

Figure 1. Schematic of apparatus.

experimental configuration used here is shown in figure 1. A supersonic jet is generated by driving the molecular gas at a pressure of one to three atmospheres through a 30 μm diaphragm, followed by a 0.5 mm diameter skimmer and two differential pumping regions. The diaphragm is located 1.2 m from the centre of the vacuum chamber, where the jet diameter is 2 mm. The background pressure in the chamber is several times 10^{-11} Torr, and the pressure rise due to the jet presence is typically 2×10^{-10} Torr. A 'catcher' pump, a 100 l s^{-1} turbomolecular pump, experiences a pressure rise of typically a 10^{-9} Torr when the jet loads it. The local pressure in the jet is typically several times 10^{-7} Torr. The laser beam, 1 cm in diameter, passes through the interaction region and is focused back onto the jet by a 10 cm focal length spherical mirror. The laser pulses are generated from a Ti:sapphire system with a pulse energy capability up to 2 mJ, a repetition rate of 2000 Hz, and central wavelength near 800 nm. Two different pulses lengths were used in this experiment: the 'long pulse' was a 25 fs pulse from the laser, lengthened to 35 fs in the interaction region by windows in the transfer system. The 'short pulse', 8 fs wide, was generated by passing the laser beam through an Ar filled fibre, negatively chirped by a set of appropriate mirrors to compensate the windows and to minimize the pulse width on the target [59]. The pulse width was measured with a Frog and checked using the known spectral yields of protons from the H_2 target [60, 61].

An electric field of 10–30 V cm^{-1} was applied at right angles to both jet and laser beam and the ions projected onto the face of a 8 cm diameter multichannel plate chevron, followed by a delay-line position-sensitive anode. The surface of the detector was 5 cm from the target focus. The position and timing signals were recorded by a sixteen-channel multi-hit time-to-digital converter and stored on an event-by-event basis for off-line analysis. A timing reference signal from the laser, as well as an amplitude signal, were obtained from a photodiode and also stored for every event. The timing precision was limited by the TDC, which has a 500 psec digitization resolution. The timing events were converted to position and flight time, and the momentum of each ion was calculated from the classical equations of motion. The kinetic energy release (KER) of each ion pair was calculated in the centre-of-mass frame, and the angle θ is that of the relative motion of the ions with respect to the polarization vector.

A typical time-of-flight spectrum is shown in figure 2 for the oxygen target, at two different laser intensities. The laser polarization vector is along the time-of-flight direction in these spectra. At this weak extraction field, the O^+ time spectrum is spread considerably by the large KER in this channel. Most of the structure seen in this non-coincident spectrum is from the dissociation channel, in which one O^+ ion and a neutral O are released, the latter going undetected. The channel on which we focus in this paper corresponds to the outermost parts

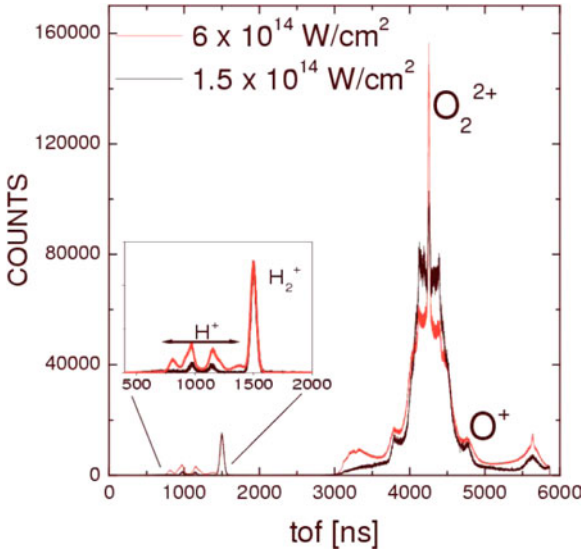

Figure 2. Time-of-flight spectrum for O_2 in 35 fs pulses at 1.5 and 6 $\times$ 10^{14} W cm^{-2} laser intensities.

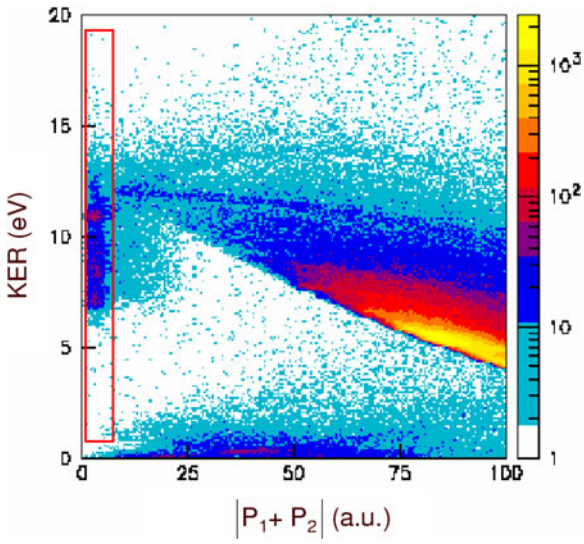

Figure 3. Density plot of the magnitude of the vector momentum sum of the two O^+ ions versus their KER.

of the O^+ group. Also visible in this spectrum are H^+ ions from a small background H_2 target, added deliberately to the system to facilitate the assignment of the laser peak intensities [62]. The laser intensities were assigned using the shape of the proton spectrum, and checked using circularly polarized light, as discussed in this reference. The peak intensities are estimated to be accurate to typically 15% for the long pulse, and to 35% for the short pulse.

Figure 3 shows a density plot of the magnitude of the vector momentum sum of the two O^+ ions versus their KER. This spectrum is used to distinguish real coincidences from random ones which result from the detection of two ions emitted from the same laser pulse but from

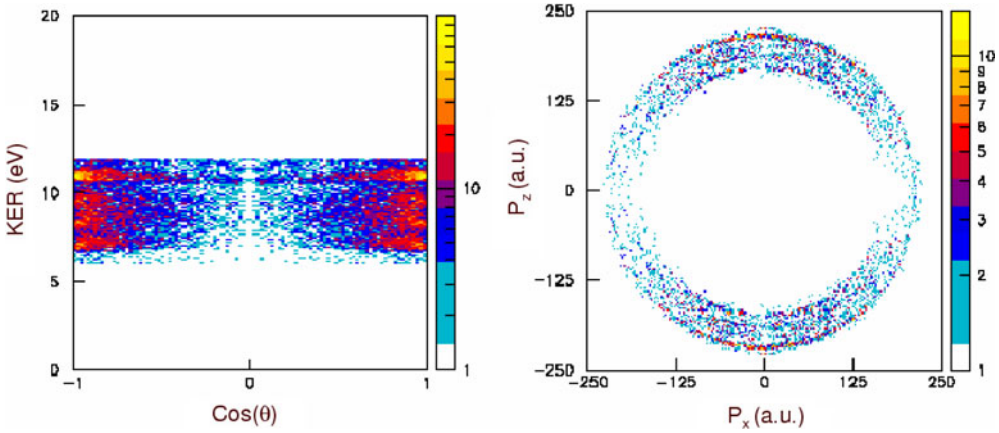

Figure 4. Density plots of spectra for O^+/O^+ coincidences for a laser intensity of 2×10^{14} W cm^{-2} and pulse length of 8 fs. The polarization vector is along the collection electric field. Left-hand panel: KER versus cos(θ). Right-hand panel: slice of the momentum sphere in the p_x–p_z plane. See text for further details.

different molecules. If the ions come from the same molecule, their total vector momentum will be near zero, and thus the real coincidences in this spectrum appear in a stripe near zero. All events for larger total momentum represent random coincidences. The advantage of this presentation is that both reals and randoms appear in the same spectrum, making it easy to see which parts of the spectrum might be subject to contamination from randoms. We select real coincidences by placing a window on the stripe near a total momentum of zero.

Figure 4 shows two different density-plot presentations of the correlated momenta for coincident O^+ ions from molecular oxygen for the data of figure 3. The left-hand panel shows a plot of the KER versus the cos(θ). Since the data can only measure the relative velocity of the oxygen ions to within an arbitrary sign, the data are reflected about cos(θ) = 0 to provide the comprehensive picture. Similar reflection is used throughout the rest of the data presentation. The gap appearing near cos(θ) = 0 results from the finite pulse-pair resolution (approximately 15 ns). The right-hand panel of figure 4 shows a slice of the 'explosion sphere' in the p_x–p_z plane, obtained by requiring that the relative momentum vector make an angle of less than 23° with respect to the x–z plane. Corresponding plots for the nitrogen target are shown in figure 5.

Results and discussion

Kinetic energy release

The KER spectra show distinct lines (left-hand panel of figure 4) or rings (right-hand panel) which correspond to discrete kinetic energy releases in the doubly charged precursor molecule. A three-dimensional momentum analysis is necessary to see this structure. If only the z-momentum spectrum is measured, as would be the case if only the times-of-flight were measured, this fine structure would be entirely washed out by the angular distribution of the fragments. Similar structure, if slightly less striking, appears for the nitrogen target in figure 5.

Figure 6 shows the corresponding KER plots for these cases. These spectra are very similar to the KER spectra seen when these molecules are dissociated by fast (200 eV) electron

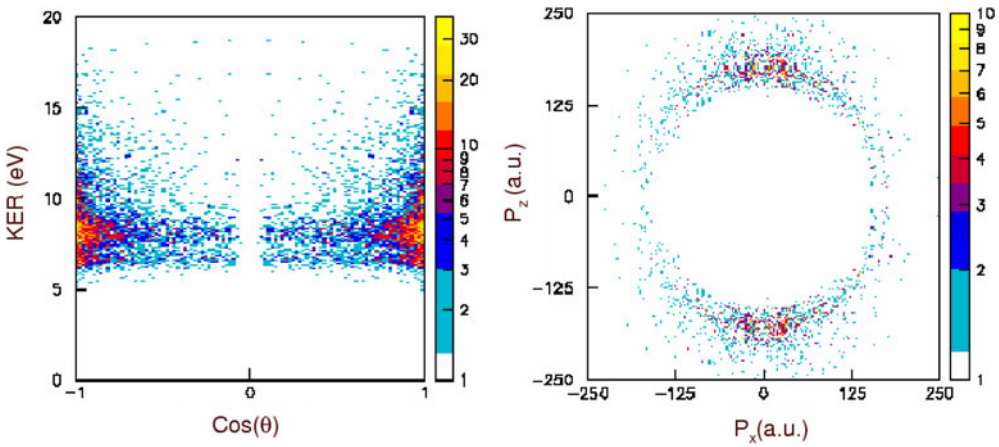

Figure 5. Similar to figure 4, but for N^+/N^+ coincidences for a laser intensity of 2.2×10^{14} W cm^{-2} and pulse length of 8 fs.

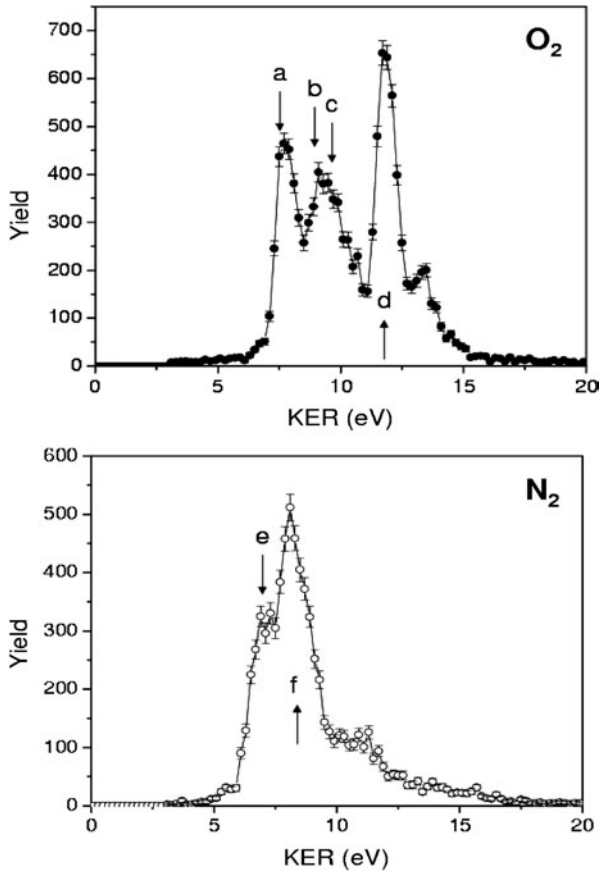

Figure 6. KER distributions for O^+/O^+ (upper) and N^+/N^+ (lower) for short pulses and intensities of 1.5 and 2 $\times$ 10^{14} W cm^{-2}, respectively. The peak identifications are labelled by letters corresponding to the states listed in table 1.

Table 1. Electronic states of the dications whose decay we observe. Adapted from [63, 64]. See those references for further details. Configurations are indicated relative to the ground state configuration of the neutral molecule.

State	Major configuration	Energy release (eV)	Final state	Figure 6
$O2\ldots\left(\ldots 3\sigma_g^2 1\pi_u^4 1\pi_g^2\right)^3\Sigma_g$				
States of O_2^{2+}				
$W^3\Delta_u$	$\pi_u{}^{-1}1\pi_g{}^{-1}$	7.2	$O^+(^4S) + O^+(^2D)$	a
$B^3\Sigma_u{}^-$	$\pi_u{}^{-1}1\pi_g{}^{-1}$	8.4	$O^+(^4S) + O^+(^2D)$	b
$1^1\Delta_u$	$\pi_u{}^{-1}1\pi_g{}^{-1}$	8.9	$O^+(^4S) + O^+(^2D)$	c
$1^1\Sigma_u{}^-$	$\pi_u{}^{-1}1\pi_g{}^{-1}$	9.7	$O^+(^4S) + O^+(^2D)$	
$B^3\Pi_g$	$3\sigma_g{}^{-1}1\pi_g{}^{-1}$	11.2	$O^+(^4S) + O^+(^4S)$	d
$1^1\Pi_g$	$3\sigma_g{}^{-1}1\pi_g{}^{-1}$	12.7	$O^+(^4S) + O^+(^4S)$	
$N_2\left(\ldots\pi_u^4 3\sigma_g^2\right)^1\Sigma_g$				
States of N_2^{2+}				
$A^1\Pi_u$	$\pi_u{}^{-1}3\sigma_g{}^{-1}$	6.9	$N^+(^3P) + N^+(^3P)$	e
$d^1\Sigma_g{}^+$	$\pi_u{}^{-2}3\sigma_g{}^{-0}$	8.6	$N^+(^3P) + N^+(^3P)$	f
$D^3\Pi_g$	$\pi_u{}^{-2}3\sigma_g{}^{-1}\,\pi_g{}^1$	8.0	$N^+(^3P) + N^+(^3P)$	

bombardment. The extremely high resolution Doppler-free measurements of Lundqvist *et al* [63, 64], combined with extensive theoretical calculations [65] allowed those authors to make unambiguous identifications of the states involved. A comparison of their KER spectra with ours reveals that the same states are being populated in the laser experiment, even with similar relative intensities. Some authors have previously used calculated potential curves for the interpretation of KER from laser induced dissociation [30, 37, 66] but the use of Coulomb potential curves remains also common. It is immediately clear that the use of Coulomb potential curves is completely unjustified in the interpretation of the decay of such a low-charge system as we are studying here. The reduction of the KER below Coulomb values has nothing to do with either dynamic screening or CREI in this case: it is simply due to the strong presence of the bonding orbitals of the molecules. This was explicitly recognized by Nibarger *et al* [30].

The ground states of O_2 and N_2 belong mainly to the configurations $\left(\ldots 3\sigma_g^2 1\pi_u^4 1p_g^2\right)^3\Sigma_g$ and $\left(\ldots\pi_u^4 3\sigma_g^2\right)^1\Sigma_g$, respectively. The ground states of the dications of these species are $\left(\ldots 3\sigma_g^2 1\pi_u^4\right)^1\Sigma_g$ and $\left(\ldots\pi_u^4\right)^1\Sigma_g$, respectively. The excited states whose decay we see correspond to excited configurations of the doubly charged ions. These states have strong configuration mixing [63–65]. In table 1 we list those states which were identified in [63, 64] and to which we attribute the major populations we see in our spectra. Since we do not resolve vibrational structure, we do not attempt to assign precise KER values to individual states but rather list in table 1 the peak locations at which we see the features indicated in our spectra. Due to the vibrational structure, each electronic state can contribute over a range of several hundred meV, depending on the shape of the potential curve in the Franck Condon region. The KER values listed correspond roughly to the average KER found in [63, 64].

Low intensity: rescattering region

We believe that the similarity of our spectra to those produced from electron bombardment is partially due to the fact that, at least for our lower intensities, the processes which create them are very similar. At laser intensities below approximately 2×10^{14} W cm^{-2} we believe we are in the 'non-sequential' regime of excitation. Non-sequential ionization is well known for

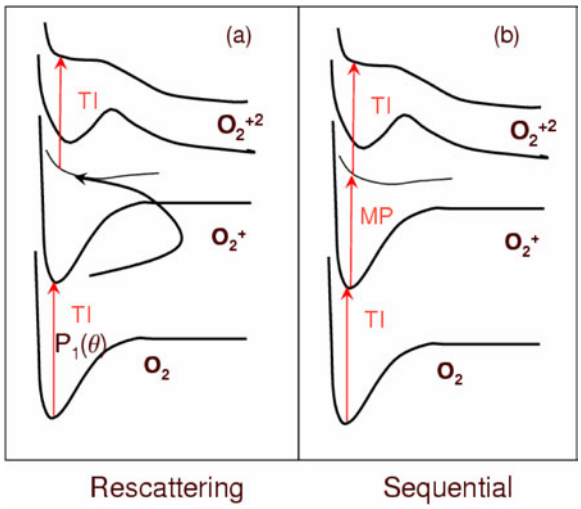

Figure 7. Schematic diagrams for (a) rescattering process and (b) sequential process.

atomic targets, and while considerable controversy over the origin of this process appeared early in the literature, it now appears that the dominant mechanism is a rescattering process: the electron released in the first ionization process returns to the parent ion with the energy it gains from the laser field and collisionally ionizes or excites this ion, leading to the production of a double charged ion. This process can be recognized experimentally either from the 'knee' in the plot of yields versus laser peak intensity or from the fact that changing from linear to circular polarization for the same peak field turns off the rescattering process. In circular polarization, the electron does not return to the parent ion.

For the case of molecules the rescattering process is less heavily studied. Recent work on H_2 has now clearly identified and characterized the process, and quantitative theoretical models have been developed which give an excellent description of the data [55, 60, 61, 67, 68]. A schematic of the rescattering process as it would apply to the molecules under discussion here is shown in figure 7(a). The initial step is a tunnelling ionization of the neutral molecule, launching both a free electron and a nuclear wave packet in the ground state potential curve of the singly charged molecular ion. The returning electron may either ionize this ion directly onto an excited molecular potential of the dication or may excite it to an excited state of the singly charged ion from which it then is quickly ionized further to the dication potential curve by the laser field.

For more complex molecules, nonsequential double ionization has been identified from both yield plots and polarization dependences [31–35, 69] for several molecules including N_2. In order to investigate whether the ion pairs we observe are generated by a rescattering process, we have investigated the dependence of these spectra on the polarization of the light. In figure 8, we plot the KER spectra for linear and circular polarization for the O_2 target. These data are taken at fixed peak field and normalized to the same number of laser pulses with the same target thickness. The upper figures, which are for low intensity, the yield is drastically reduced when the laser is circularly polarized, a result which we interpret to mean that the operating mechanism for double ionization includes a rescattering step. A similar result is also shown for N_2 in figure 8. This result is in agreement with the expectation from [31–35], which show the transition from non-sequential (rescattering) to sequential ionization to occur in the range of 2–4 $\times$ 10^{14} W cm^{-2}. The exact transition intensity is species dependent.

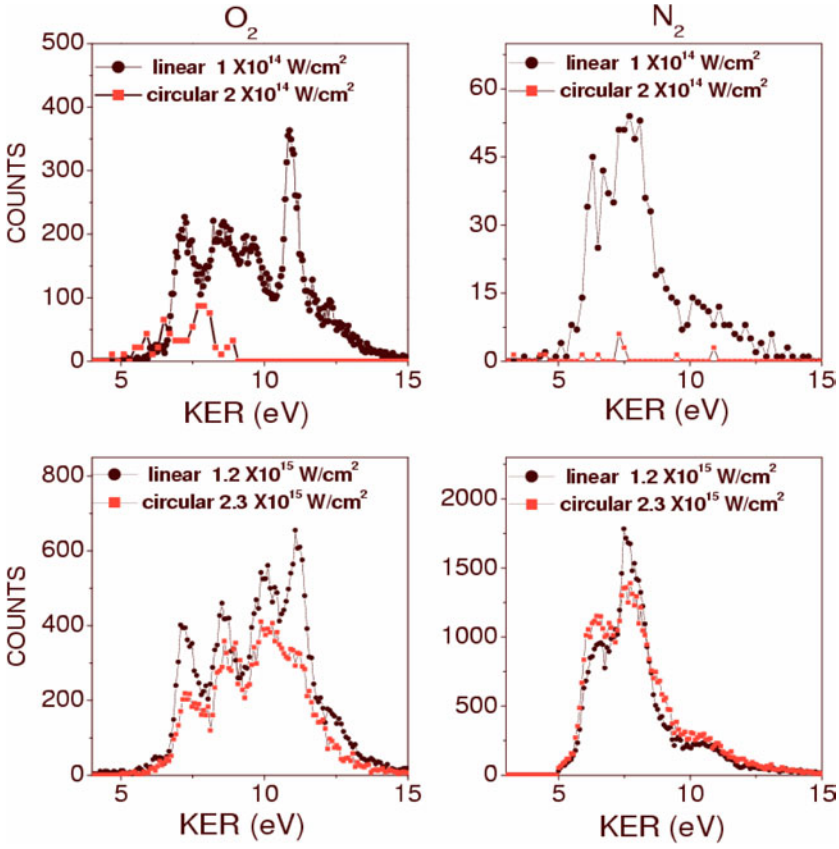

Figure 8. A comparison of KER spectra for linear and circular polarization for oxygen (left column) and nitrogen (right column). The spectra are normalized to approximately the same number of laser pulses and for the same target densities. The pulse length is 30 fs for the first row, and 8 fs for the second row.

In the rescattering process, the energy of the returning electron at an intensity of 1×10^{14} W cm^{-2} is at most 20 eV. This is insufficient to ionize the ground state of the singly charged ions directly into the states we see. However, we know from the H_2 case that it is very likely for a double step process to occur: the returning electron excites the singly charged molecule, which is then quickly ionized by the laser field. We envision in this case that the double ionization begins by forming the $\left(\ldots 3\sigma_g^2 1\pi_u^4 1\pi_g^1\right) X\,^2\Pi_g$ (oxygen) or $\left(\ldots \pi_u^4 3\sigma_g^1\right) X\,^2\Sigma_g^+$ (nitrogen) ground states of the singly charged molecule by removing the outer electron from the neutral. The returning electron then excites an 'inner' valence electron from the $3\sigma_g$ or $1\pi_u$ orbital into a higher orbital, forming an excited state of the singly charged molecular ion from which further ionization into the continuum occurs rapidly. As long as 'inner' valence orbitals are involved, both triplet and singlet final states can be formed by this process, as is observed experimentally. We do not presume to propose an exact pathway for this process at this point. The exact ionization mechanisms for the free electron and laser cases, while similar in nature, are rather different in detail, and one thus is not surprised to find differing intensity ratios for the states created. The absence of states in our spectra for KER above about 14 eV, which are strongly populated by the high energy free electrons, is possibly due to the much lower energy of the 'bombarding' electrons in the laser case.

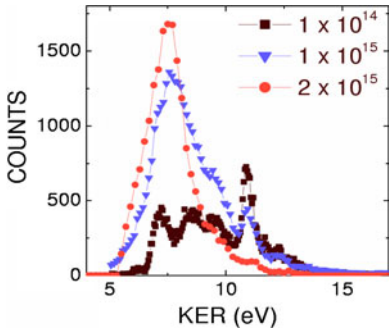

Figure 9. Evolution of KER spectrum for oxygen in the 35 fs pulses as the laser intensity is raised.

Sequential region

As the laser intensity is raised, going from linear to circular polarization no longer causes the ion-pair yield to decrease. The lower panels of figure 8 show a comparison of KER spectra for linearly and circularly polarized light in this higher intensity region. We choose to display data at high intensities mainly for the short pulse here, for reasons we discuss below. We believe that, at the higher intensity, the ionization proceeds through a sequential process, shown schematically in figure 7(b), whereby the tunnelling ionization of the neutral molecule to the singly charged one is followed some time later by tunnelling ionization of the singly charged ion to the doubly charged one. We emphasize that the ionization steps must also be accompanied by a third step which electronically excites the molecule, since otherwise one ends up on the $\left(\ldots 3\sigma_g^2 1\pi_u^4\right)^1\Sigma_g$ (oxygen) or $\left(\ldots \pi_u^4\right)^1\Sigma_g$ (nitrogen) potential curve of the dication which is metastable and which gives rise to undissociated doubly charged molecules. At least two candidates are available for the electronic excitation: multiphoton excitation by the laser field, often discussed in terms of bond softening [70, 71], and inner electron ionization [72, 73]. We do not pretend at this point to be able to determine what is occurring here. The multiphoton process could occur in either the neutral or the singly charged ion. We note that we produce both singlet and triplet final states of the dication, so multiphoton excitation from the ground state of the dication cannot be the explanation. At least one 'inner' orbital must be involved in whatever process produces the final dissociating state.

Why do we choose to present KER spectra in the sequential region (above 4×10^{14} W cm^{-2}) for the short pulse case in figure 8? Because for the case of O_2 the KER spectra substantially change their nature in this region when longer pulses are used. In figure 9 we show the evolution of the O_2 KER spectrum in 35 fs laser pulses as the intensity is raised. The sharp structures seen in the rescattering region are progressively lost, and the centroid of the KER spectrum shifts to smaller values. We interpret this effect as due to the time which may elapse between the first and second stages of ionization. The equilibrium distance of the O_2^+ molecule (2.11 au) is slightly less than that of the O_2 molecule (2.30 au), so removing one π_g electron from the neutral molecule should launch a wave packet in the ground state potential of the O_2^+ ground state potential. This wave packet will both move and spread, the latter probably being the more important effect here, with a period near 20 fs, and if the second ionization occurs with a delay of this magnitude, a vertical transition is no longer the correct description. This can easily occur for a pulse length of 35 fs. A spread of internuclear distances in the wave packet in the O_2^+ potential will produce a spread of KER of the final fragments through reflection onto the final repulsive curves through which the breakup occurs. That the average KER seems to decrease as the laser intensity is increased may result from the

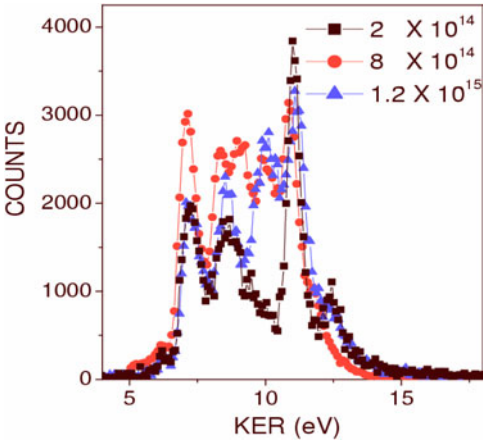

Figure 10. Evolution of KER spectrum for oxygen in the 8 fs pulses as the laser intensity is raised.

increase of the second ionization rate with increasing internuclear distance. One is beginning to see CREI-like dissociation characteristics. We note that such a spreading caused by a delay between ionization steps is improbable for the rescattering process, because only the first three cycles or so after the emission of the electron are likely to be effective in the next step. This limits the possible delay to about 8 fs [60, 61, 67, 68].

The KER spectra for N_2 do not show this loss of resolution with increasing laser intensity. This may be due to the fact that the equilibrium distances, and even the vibrational spacings, for the ground state potentials of N_2 and N_2^+ are nearly identical (2.07 au). Thus it is possible that the wave packet launched into the N_2^+ well is also nearly stationary, and no spread of internuclear distances ensues.

If the above explanation for O_2 is correct, one would expect that one might remove the spreading of the KER by using pulses so short that the internuclear distance is essentially frozen. Figure 10 shows that this is indeed the case. When an 8 fs pulse with an intensity of 1.2×10^{15} W cm^{-2} is used, well into the sequential region, the sharply defined structure in the KER spectrum is regained. It is interesting that the KER spectrum is so similar to that for the rescattering region, since the mechanism for producing it is quite different. A similar result is seen for N_2, but since here no washing out was seen for the 'long' pulse, there is no resolution to recover.

Angular distributions

In an earlier publication [56] we showed that the angular distributions in the rescattering region, at the lowest intensities, are very different for oxygen and nitrogen. This is apparent already from figures 3 and 4, and is summarized again in figure 11, where we show polar plots of the angular distributions for several representative KER for both molecules. The oxygen molecules tend to maximize at around 40° to the polarization vectors, while the nitrogen molecules maximize at zero degrees. As discussed in [56], we interpret this to be due to the angular distribution $P_1(\theta)$ of the first step of the rescattering ionization process (figure 7). The molecular ADK tunnelling calculations of Tong *et al* [39] predict that this angular distribution should reflect the symmetry of the most loosely bound orbital of the molecule, which for oxygen is a π_g while for the nitrogen it is a σ_g. The shapes of these orbitals are

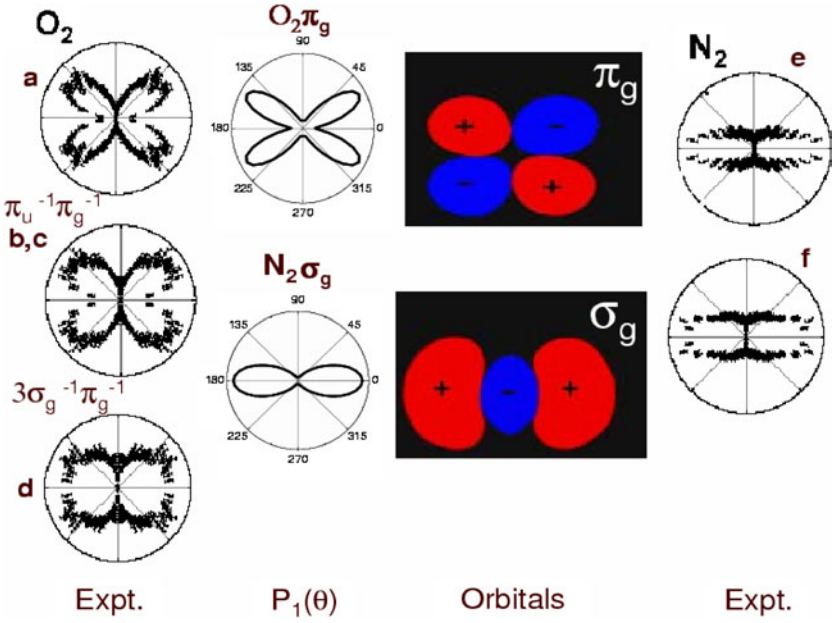

Figure 11. Polar plots of angular distributions of O^+/O^+ (left-hand column) and N^+/N^+ (right-hand column) distributions as a function of θ for different peaks in the KER spectrum of figure 6. These data are for the lowest intensity and shortest pulse length, and show the angular patterns expected for the first ionization stage from the molecular ADK tunnelling theory. These theoretical patterns, $P_1(\theta)$, and the orbitals whose structure they reflect, are shown schematically in the central columns.

shown schematically in figure 11, along with the predictions for $P_1(\theta)$. These shapes are seen to have a remarkable similarity to the observed angular distributions.

Our initial measurements did not show such striking results, and it was only by using the 8 fs pulse and the lowest intensities that these simple angular distributions were observed. Both the laser peak intensity and the pulse length were found to have substantial effects on the observed angular distributions. Figure 12 shows polar plots of the angular distributions for peak (a), the $W^3\Delta_u\left(\pi_u^{-1}1\pi_g^{-1}\right)$ state (where the configuration is expressed relative to that of the neutral molecule), of the dication for the short pulse for different laser intensities. Similar distributions are seen for peaks (b) and (c), which have similar main configurations. The clover-leaf pattern remains as the laser intensity is raised but the whole pattern closes slowly towards zero degrees. At the highest intensity, peaking at zero degrees becomes so marked that this clover structure is lost entirely. Figure 13 shows the corresponding plots for the 35 fs pulse case, where the closing of the pattern towards zero degrees is present even for the lowest intensity measured.

It is known that, for the intensities used here, the periods of pendular states of these molecules, calculated from the ground state polarizibilities of the molecules, are in the several hundred femtosecond range. Thus one would not immediately expect that significant alignment of the molecule over the short times of the pulses used here could appear. However, distortion of the angular distributions is still possible, even though very little actual alignment is realized. Tong *et al* [74] have evaluated this possibility quantitatively using time-dependent polarizabilities, and found that the folding of the clover-leaf pattern towards zero degrees with increasing intensity appears to be a natural consequence of the tendency of the molecules to seek, if not fully to realize, alignment during the pulse. Of course, as the laser intensity is

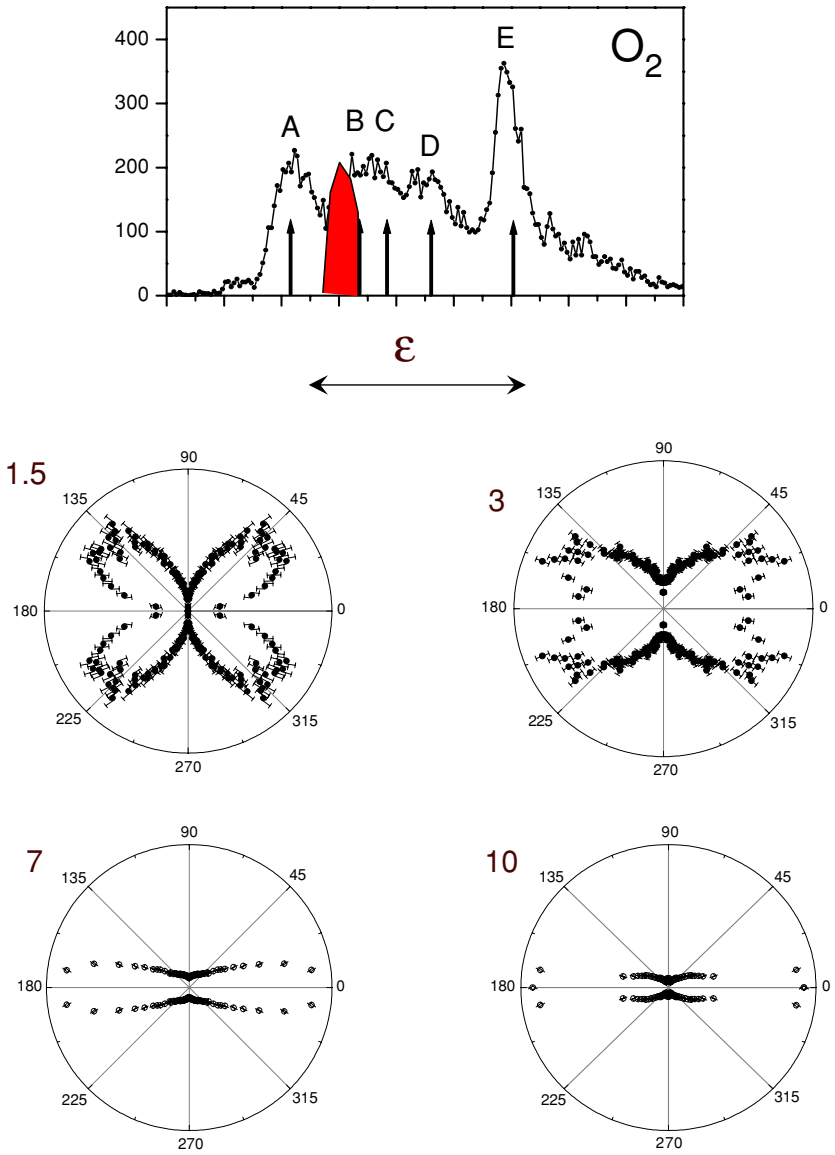

Figure 12. Evolution of the angular distributions for π_g removal (peak (a) in table 1) for different intensities for O^+/O^+. The laser peak intensity in units of 10^{14} W cm^{-2} is shown beside each plot. The pulse length is 8 fs.

raised into the sequential region, the whole process also changes character, and the loss of the clover-leaf pattern might well be due to the influence of angular distributions of the other steps involved in the double ionization/excitation process.

Figures 14 shows the short-pulse angular distribution for the (E), the $B^3\Pi_g$ $\left(3\sigma_g^{-1}1\pi_g^{-1}\right)$, state of the dication of oxygen. The angular distribution for this state shows a much weaker clover-leaf pattern than do states (a)–(c), and shows additional anomalous behaviour as discussed further below. We suspect that this result is associated with the necessity to produce a $3\sigma_g$ hole for its population. If its production requires the extraction of the 'inner' valence

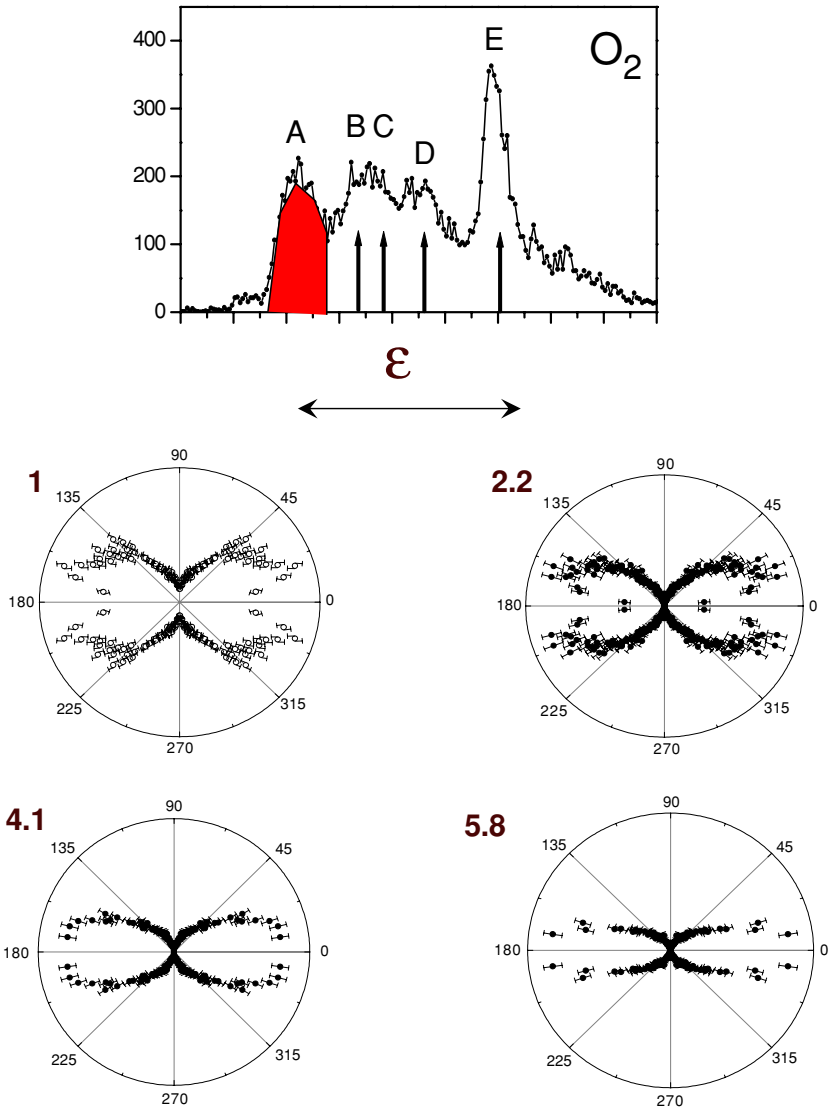

Figure 13. The same as figure 12 except for the 35 fs pulse.

$3\sigma_g$ electron in the first tunnelling step, then the tendency to peak more at zero degrees is natural, since the molecular ADK prediction predicts zero degree peaking for ionization of this orbital. As the intensity increases, this state shows even stranger behaviour: a subordinate peak begins to grow at $\theta = 90^\circ$, as is seen in figure 14. This effect is not seen for any state with the nitrogen target, for which all observed angular distributions peak at zero degrees with no subordinate side lobes. For nitrogen we see increasingly sharp peaking at zero degrees as the intensity of the laser is raised, for both short and long pulses. One is thus led to seek a process which favours the alignment of the molecule at right angles to the polarization vector. Such a process would be a bond-softening/multi-photon π_g to σ_u transition, which would require that an odd number of 'π' photons be absorbed. (By the notation 'π' photons, we

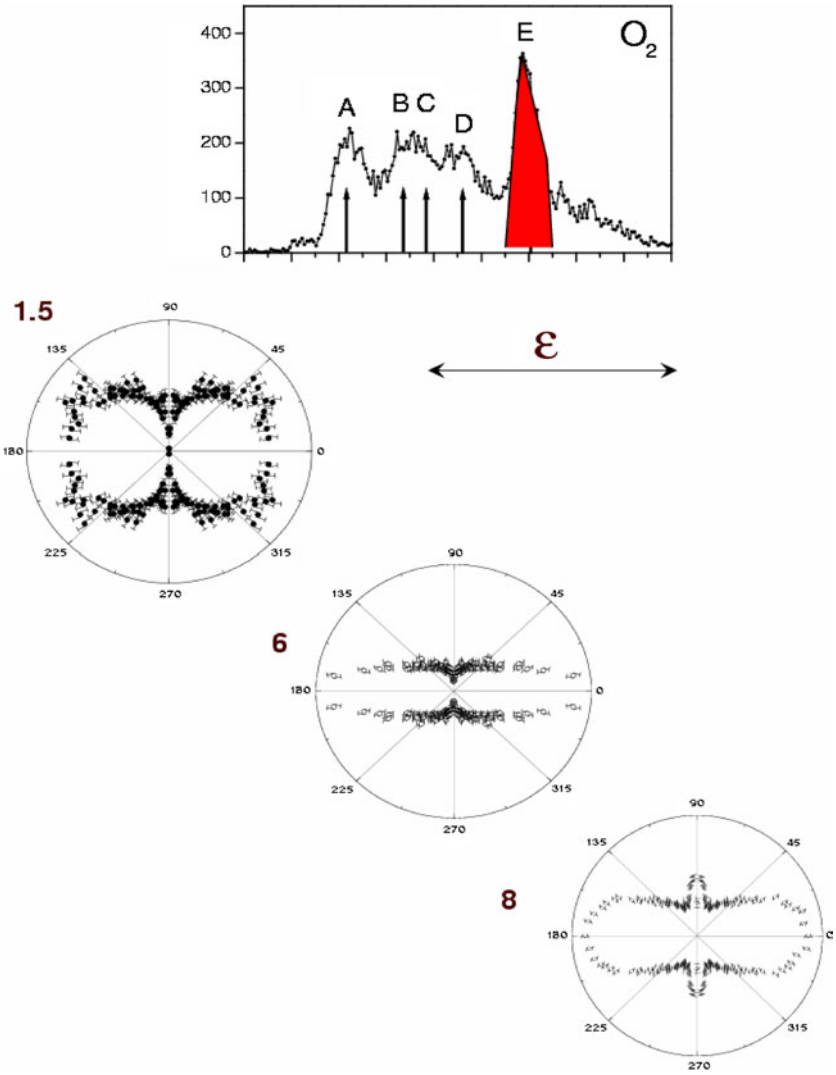

Figure 14. The same as figure 12 but for $3\sigma_g$ removal (peak (e) in table 1).

mean photons with polarization at right angles to the internuclear axis). In the absence of real potential curves, we discuss this possibility in terms of the underlying molecular orbitals which could be populated by such a process. Within the valence basis set having only $1\pi_u$, $3\sigma_g$ and π_g orbitals no such transition is available, but if the $3\sigma_u$ orbital, which is energetically the next one expected, is added to the set, such a transition becomes possible. This orbital is not bound in the neutral molecule, but is in the dication and could be at least resonantly populated in the singly charged ion. The excitation through a bond-softening process of a state with population in such an orbital would require the absorption of at least 10 eV, that is five to seven photons, but is entirely possible for our highest intensities. Of course, the actual eigenstates of the molecule have considerable configuration mixing, and the population of this configuration would be expected to affect more than a single final state. Indeed, the 90° peak seen for the (E) state in figure 14 is seen to a lesser extent for other states. In figure 15

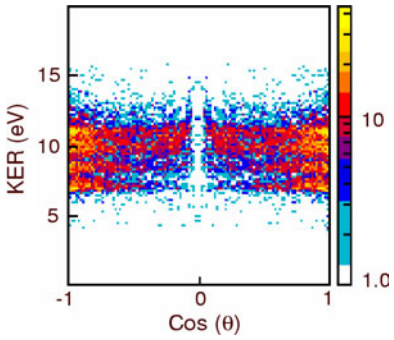

Figure 15. KER versus cos(θ) at 8×10^{14} W cm^{-2}, 8 fs pulse, oxygen.

we show a KER versus cos(θ) plot for the short pulse at 8×10^{14} W cm^{-2} laser intensity. A tendency for peaking at 90° is seen for the (E) state with a KER of 11 eV, but is also seen more weakly for other states.

Summary

By using full momentum imaging of singly charged ion pairs produced by dissociating nitrogen and oxygen by short laser pulses, we have observed and identified the electronic states of the dications of these species through which the double ionization/fragmentation process occurs. The KER spectra are very similar to those produced by electron bombardment of the same molecules. Two different ionization mechanisms were identified. For low intensity and 'long' pulses (35 fs), rescattering dominates. This was verified by comparing KER spectra produced with linear and circular polarization. As the laser intensity is raised, one enters the non-sequential regime, there the polarization dependence vanishes. Features in the KER spectrum corresponding to resolved electronic states of the dication become washed out. We attribute this to the time delay which occurs between the first and second steps of ionization in the sequential regime. This conjecture was tested by subjecting the molecules to pulses of similar intensity but 'short' (8 fs). The shortness of the pulses now 'freezes' the internuclear motion and the resolution of well-defined features in the KER spectra is recovered.

Our data show clearly that the use of Coulomb potential curves for the discussion of the KER spectra is not appropriate or even very relevant to such low-charged molecules. This observation is likely to be valid to a lesser degree for even higher charged molecules. Some care should probably be taken before drawing too many quantitative conclusions about the dissociation mechanisms for molecules exploded by short fast laser pulses unless some attempt to evaluate the effects of the populated bonding orbitals is taken into account.

Acknowledgments

This work was supported by Chemical Sciences, Geosciences and Biosciences Division, Office of Basic Energy Sciences, Office of Science, US Department of Energy. The laser facility was partially supported by an NSF MRI grant. We thank A Bandrauk for suggesting the possible importance of bond softening transitions at 90°, and P Corkum and H Staplefeld for stimulating discussions concerning the role of molecular alignment in the field.

References

[1] Nibarger J P, Menon S V and Gibson G N 2001 *Phys. Rev.* A **63** 053406
[2] Codling K, Cornaggia C, Frasinski L J, Hatherly P A, Morellec J and Normand D 1991 *J. Phys. B: At. Mol. Opt. Phys.* **24** L593
[3] Cornaggia C, Lavancier J, Normand D, Morellec J, Agostini P, Chambaret J P and Antonetti A 1991 *Phys. Rev.* A **44** 4499
[4] Posthumus J H, Codling K, Frasinski L J and Thompson M R 1997 *Laser Phys.* **7** 813
[5] Gibson G N, Li M, Guo C and Nibarger J P 1998 *Phys. Rev.* A **58** 4723
[6] Nibarger J P, Li M, Menon S and Gibson G N 1999 *Phys. Rev. Lett.* **83** 4975
[7] Quaglia L and Cornaggia C 2000 *Phys. Rev. Lett.* **84** 4565
[8] Hishikawa A, Iwamae A, Hoshina K, Kono M and Yananouchi K 1998 *Chem. Phys.* **231** 315
[9] Boyer K, Luk T S, Solem J C and Rhodes C K 1989 *Phys. Rev.* A **39** 1186
[10] Dietrich P, Strickland D T and Corkum P B 1993 *J. Phys. B: At. Mol. Opt. Phys.* **26** 2323
[11] Strickland D T, Beaudoin Y, Dietrich P and Corkum P B 1992 *Phys. Rev. Lett.* **68** 2755
[12] Codling K, Cornaggia C, Frasinski L J, Hatherly P A, Morellec J and Normand D 1991 *J. Phys. B: At. Mol. Opt. Phys.* **24** L595
[13] Iwamae A, Hisikawa A and Yamanouchi K 2000 *J. Phys. B: At. Mol. Opt. Phys.* **33** 223
[14] Kawata I, Kono H, Fujimura Y and Bandrauk A D 2000 *Phys. Rev.* A **62** 031401 (R)
[15] Barnett R and Gibson G N 1999 *Phys. Rev.* A **59** 4843
[16] Saenz A 2000 *Phys. Rev.* A **61** 051402
[17] Zuo T, Chelkowski S and Bandrauk A D 1993 *Phys. Rev.* A **48** 3837
[18] Bandrauk A D 2000 *The Physics of Electronic and Atomic Collisions AIP Conf. Proc.* vol 500 ed Y Itikawa *et al* (New York: AIP) p 102
[19] Codling K, Posthumus J H and Frasinski L J 2000 *The Physics of Electronic and Atomic Collisions* AIP Conf Proc. vol 500 ed Y Itikawa *et al* (New York: AIP) p 3
[20] Constant E, Stapelfeldt H and Corkum P B 1996 *Phys. Rev. Lett.* **76** 4140
[21] Gibson G N, Li M, Guo C and Neira J 1997 *Phys. Rev. Lett.* **79** 2022
[22] Posthumus J H, Frasinski L J, Giles A J and Codling K 1995 *J. Phys. B: At. Mol. Opt. Phys.* **28** L349
[23] Seideman T, Yu Ivanov M and Corkum P B 1995 *Phys. Rev. Lett.* **75** 2819
[24] Zuo T and Bandrauk A D 1995 *Phys. Rev.* A **52** R2511
[25] Brewczyk M, Rzazewski K and Clark C W 1997 *Phys. Rev. Lett.* **78** 191
[26] Hering Ph, Brewczyk M and Cornaggia C 2000 *Phys. Rev. Lett.* **85** 2288
[27] Brewczyk M and Rzazewski K 2000 *Phys. Rev.* A **61** 023412
[28] Cornaggia C, Lavancier J, Normand D, Morellec J and Liu H X 1990 *Phys. Rev.* A **42** 5464
[29] Cornaggia C, Normand D and Morellec J 1992 *J. Phys. B: At. Mol. Opt. Phys.* **25** L415
[30] Nibarger J P, Menon S V and Gibson G N 2001 *Phys. Rev.* A **63** 053406
[31] Guo C, Li M, Nibarger J P and Gibson G N 2000 *Phys. Rev.* A **61** 033413
[32] Guo C and Gibson G N 2003 *Phys. Rev.* A **63** 040701
[33] Cornaggia C and Hering Ph 1998 *J. Phys. B: At. Mol. Opt. Phys.* **31** L503
[34] Guo C, Li M, Nibarger J P and Gibson G N 1998 *Phys. Rev.* A **58** R4271
[35] Cornaggia C and Hering Ph 2000 *Phys. Rev.* A **62** 023403
[36] Chelkowski S and Bandrauk A D 1995 *J. Phys. B: At. Mol. Opt. Phys.* **28** L723
[37] Bandrauk A D, Musaev D G and Morokuma K 1999 *Phys. Rev.* A **59** 4309
[38] Ammosov M V, Delone N B and Krainov V P 1986 *Zh. Eksp. Teor. Fiz.* **91** 2008
Ammosov M V, Delone N B and Krainov V P 1986 *Sov. Phys.—JETP* **64** 1191
[39] Tong X M, Zhao Z X and Lin C D 2002 *Phys. Rev.* A **66** 033402
[40] Talebpour A, Larochelle S and Chin S L 1998 *J. Phys. B: At. Mol. Opt. Phys.* **31** L49
[41] Guo D S, Freeman R R and Wu Y S 1998 *Phys. Rev.* A **58** 521
[42] DeWitt M J, Wells E and Jones R R 2001 *Phys. Rev. Lett.* **87** 153001
[43] Wells E, DeWitt M J and Jones R R 2002 *Phys. Rev.* A **66** 013409
[44] Talebpour A, Chien C-Y and Chin S L 1996 *J. Phys. B: At. Mol. Opt. Phys.* **29** L677
[45] Guo C, Li M, Nibarger J P and Gibson G N 1998 *Phys. Rev.* A **58** R4271
[46] DeWitt M J and Levis R J 1998 *J. Chem. Phys.* **108** 7739
[47] Saenz A 2000 *J. Phys. B: At. Mol. Opt. Phys.* **33** 4365
[48] Guo C 2000 *Phys. Rev. Lett.* **85** 2276
[49] Muth-Böhm J, Becker A and Faisal F H M 2000 *Phys. Rev. Lett.* **85** 2280
[50] Muth-Böhm J, Becker A, Chin S L and Faisal F H M 2001 *Chem. Phys. Lett.* **337** 313

[51] Staplefeld H and Seideman T 2003 *Rev. Mod. Phys* **75** 543
[52] Litvinyuk I V *et al* 2003 *Phys. Rev. Lett.* **90** 233003
[53] Légaré F *et al* 2004 Private communication
[54] Staudte A *et al* 2002 *Phys. Rev.* A **65** 020703(R)
[55] Alnaser A S *et al* 2003 *Phys. Rev. Lett.* **91** 163002
[56] Alnaser A S *et al* 2004 *Phys. Rev. Lett.* **93** 113003
[57] Ullrich J *et al* 1997 *J. Phys. B: At. Mol. Opt. Phys.* **30** 2917
[58] Dörner R *et al* 2000 *Phys. Rep.* **330** 95
[59] Nisoli M *et al* 1997 *Opt. Lett.* **22** 522
[60] Tong X M, Zhao X and Lin C D 2003 *Phys. Rev. Lett.* **91** 233203
Tong X M and Lin C D 2004 *Phys. Rev.* A **70** 023406
[61] Alnaser A S *et al* 2004 *Phys. Rev. Lett.* at press
[62] Alnaser A S *et al* 2004 *Phys. Rev.* A **70** 023413
[63] Lundqvist M, Edvardsson D, Baltzer P, Larsson M and Wannberg B 1996 *J. Phys. B: At. Mol. Opt. Phys.* **29** 499
[64] Lundqvist M, Edvardsson D, Baltzer P and Wannberg B 1996 *J. Phys. B: At. Mol. Opt. Phys.* **29** 1489
[65] Larsson M, Baltzer P, Svensson S, Wannberg B, Maartensson N, Naves de Brito A, Correia N, Keans M P, Carlsson-Goethe M and Karlsson L 1990 *J. Phys. B: At. Mol. Opt. Phys.* **23** 1175
[66] Hill W T, Zhu J, Hatten D L, Cui Y, Boldhar J and Yang S 1992 *Phys. Rev. Lett.* **69** 2646
[67] Niikura H *et al* 2002 *Nature* **417** 917
[68] Niikura H, Légaré F, Hasbani R, Yu Ivanov M, Villeneuve D M and Corkum P B 2003 *Nature* **421** 826
[69] Hering Ph and Cornaggia C 1998 *Phys. Rev.* A **59** 2836
[70] Zavriyev A, Bucksbaum P H, Muller H G and Schumacher D W 1990 *Phys. Rev.* A **42** 5500
[71] Zavriyev A, Bucksbaum P H, Squier J and Saline F 1993 *Phys. Rev. Lett.* **70** 1077
[72] Tablepour A, Bandrauk A D, Vijayalakshimi K and Chin S L 2000 *J. Phys. B: At. Mol. Opt. Phys.* **33** 4615
[73] Chu X and Chu Sh-I 2001 *Phys. Rev.* A **64** 063404
[74] Tong X-M *et al* 2004 submitted